



ChemComm

**Highly Selective CO₂ Removal for One-Step Liquefied
Natural Gas Processing by Physisorbents**

Journal:	<i>ChemComm</i>
Manuscript ID	CC-COM-01-2019-000626.R1
Article Type:	Communication

SCHOLARONE™
Manuscripts

Highly Selective CO₂ Removal for One-Step Liquefied Natural Gas Processing by Physisorbents

Received 00th January 20xx,
Accepted 00th January 20xx

David G. Madden^a, Daniel O’Nolan^a, Kai-Jie Chen^a, Carol Hua^a, Amrit Kumar^a, Tony Pham^b, Katherine A. Forrest^b, Brian Space^b, John J. Perry IV^a, Majeda Khraisheh^c, Michael J. Zaworotko^{a*}

DOI: 10.1039/x0xx00000x

www.rsc.org/

Industrial specifications require CO₂ concentrations in natural gas of below 50 ppm during liquefaction because of corrosion and CO₂ freezing. Herein, we report a physisorbent (TIFSIX-3-Ni) that exhibits new benchmark CO₂/CH₄ selectivity and fast kinetics, thereby enabling one-step LNG processing to CO₂ levels of 25 ppm.

Methane, CH₄, is the main component of natural gas (NG) and other fuel sources such as biogas and landfill gas. Its importance is heightened as we are now at the dawn of the “Age of Gas”¹ whereby new technologies develop around the use of gases as either fuels or feedstock chemicals. Indeed, in 2016, around 30% of global energy was produced by power stations burning NG² and this is expected to rise 45% by 2040.³ Rising global consumption of NG has led to a significant increase in demand for liquefied NG (LNG), the highest energy density form of NG for transportation.³ Global LNG demand is projected to more than double from 8 trillion cubic feet in 2008 to 19 trillion cubic feet by 2035.⁴ Industrial specifications require CO₂ concentrations in NG of <50 ppm during liquefaction because of corrosion and CO₂ freezing at -161 °C⁶⁻⁸. Currently, CO₂ is removed from NG to 50 ppm *via* liquid amine chemisorption, however, this NG must be processed several times to realise LNG grade purity.⁹ Regenerating liquid amines is also energy intensive, reducing the overall efficiency of the process.⁷

Physisorption offers promise to greatly improve the energy efficiency of small molecule industrial gas separations.¹⁰ This is because solid physisorbents are generally less toxic and volatile, more robust, and easier to regenerate than chemisorbents. Though much has been done in the context of solid physisorbents and membranes for upgrading natural gas,

landfill gas and biogas,^{7, 11-13} we are unaware of any studies that specifically address reducing the CO₂ concentration of NG to <50 ppm from CO₂ concentrations representative of NG mixtures (<2% in coal seam methane reserves, *ca.* 15% in Australia and >50% in stranded gas fields).¹⁴ In this contribution, we investigate six physisorbents that exhibit high CO₂/CH₄ selectivity, *S*_{CM}, for their utility in both trace (1%) and bulk (50%) CO₂ removal from simulated NG mixtures. The six materials studied herein represent three classes of physisorbents that have been generally studied for carbon capture: four hybrid ultramicroporous materials, HUMs (TIFSIX-3-Ni (Figure 1), SIFSIX-3-Ni, TIFSIX-2-Cu-i and NbOFFIVE-1-Ni)¹⁵⁻¹⁸; a MOF (Mg-MOF-74)¹⁹; a zeolite (Zeolite 13X)^{20, 21}. Mg-MOF-74 and Zeolite 13X are considered the current benchmark physisorbents for CO₂/CH₄ separations in terms of both *S*_{CM} and working capacity.^{7, 22} The performance of the six sorbents was evaluated from single-component gas adsorption isotherms, molecular dynamics simulations, dynamic gas mixture breakthrough experiments and gravimetric gas uptake experiments.

The single component gas adsorption isotherms of the six physisorbents were collected for CO₂ and CH₄ (Fig. 2A) at 298 K. The CO₂ uptake observed for each physisorbent is consistent with previous reports.^{15-21, 23, 24} At 1.0 bar, Mg-MOF-74 exhibits the highest CO₂ sorption capacity (7.0 mmol g⁻¹), while the HUMs exhibit much the highest CO₂ uptakes at low CO₂ partial

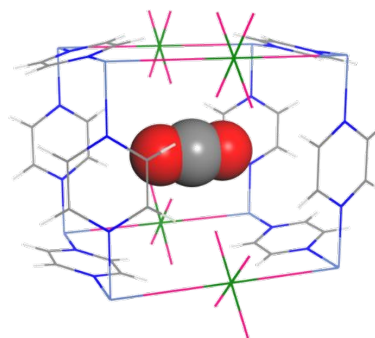


Figure 1. CO₂ loaded structure of TIFSIX-3-Ni (CO₂@TIFSIX-3-Ni) topology as obtained from *in-situ* synchrotron PXRD.

^a Bernal Institute, Department of Chemical Sciences, University of Limerick, Limerick, Republic of Ireland.

^b Department of Chemistry, University of South Florida, 4202 East Fowler Avenue, CHE205, Tampa, Florida 33620, United States.

^c Department of Chemical Engineering, College of Engineering, Qatar University, Doha, Qatar.

Electronic Supplementary Information (ESI) available: See DOI: 10.1039/x0xx00000x

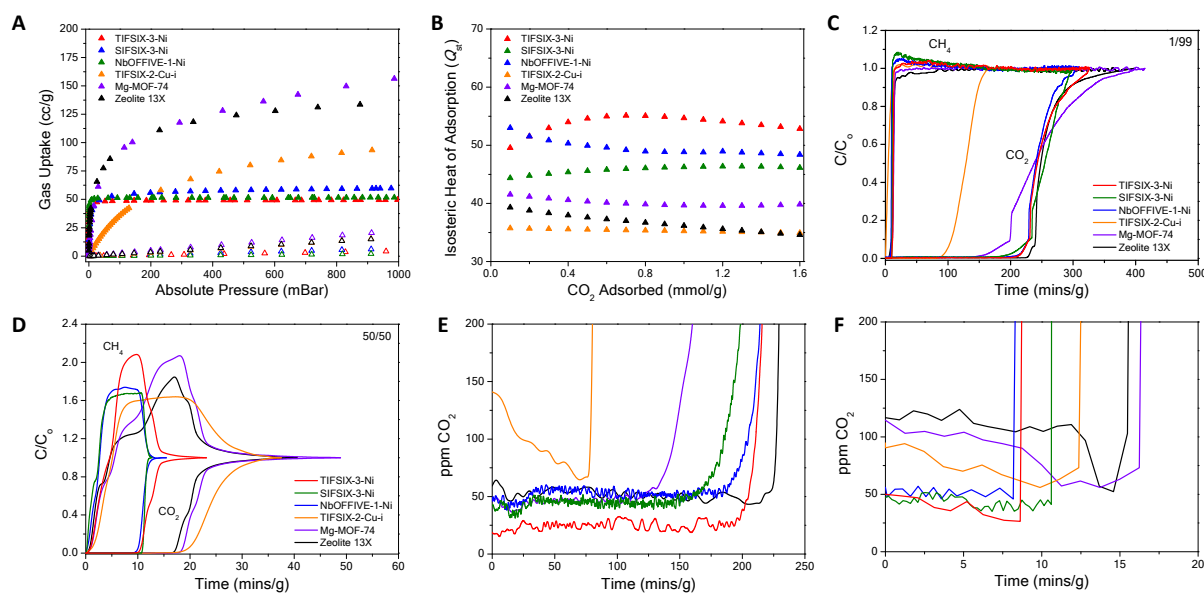


Figure 2. A, Low pressure CO₂ (Solid Triangles) and CH₄ (Open Triangles) isotherms at 298 K. B, CO₂ isosteric heats of adsorption. C, 1% CO₂/99% CH₄ and D, 50% CO₂/50% CH₄ gas mixture breakthrough curves. CO₂ effluent concentrations for E, 1% CO₂/99% CH₄ and F, 50% CO₂/50% CH₄ gas mixtures.

pressures (<4 mBar). The isosteric heat of adsorption (Q_{st}) for CO₂ at low coverage (Fig. 2B) is ordered as follows: **NbOFFIVE-1-Ni** (54 kJ mol⁻¹) > **TIFSIX-3-Ni** (50 kJ mol⁻¹) > **SIFSIX-3-Ni** (45 kJ mol⁻¹) > **Mg-MOF-74** (42 kJ mol⁻¹) > **Zeolite 13X** (39 kJ mol⁻¹) > **TIFSIX-2-Cu-i** (35.8 kJ mol⁻¹).²¹ These Q_{st} values indicate that the CO₂ uptake at low partial pressures correlates with the strength of sorbent-sorbate interactions. In contrast, each sorbent exhibits much lower CH₄ uptake at 1.0 bar and 298 K (Fig. 2A and Table 1).

The CO₂ binding site in isostructural HUMs has previously been identified through *in situ* crystallographic experiments (Supporting Information, Fig. S54) and molecular modelling (Fig. S23-S24);^{12, 17, 25} CO₂ molecules lie in the plane of the equatorial fluorine atoms that afford strong F⁻CO₂ electrostatics. Molecular dynamics simulations indicate that CH₄ adsorbs in HUMs such that CH₄ molecules also interact with the negatively charged inorganic pillars (SiF₆²⁻ and TiF₆²⁻) (Fig. S21-S22), in this case through multiple weak F⁻H interactions. That CO₂ is adsorbed in HUMs through multiple stronger F⁻CO₂ interactions results in significantly higher energies than those that accompany CH₄ adsorption, which, at 25-30 kJ/mol (Table S7), are relatively high,²⁵ but nevertheless much lower than those associated with CO₂ adsorption.

Analysis of the pure gas isotherms *via* ideal adsorbed solution theory (IAST)²⁶ provided estimated S_{CM} values under relevant conditions (298K; CO₂ mole fractions of 0.01 and 0.5) and the extreme range of compositions of NG (Fig. S18-S19 and Table 1). **NbOFFIVE-1-Ni** and **TIFSIX-3-Ni** were found to exhibit new benchmarks for S_{CM} (8482 and 3501, respectively), values far above those of previously reported sorbents (**SIFSIX-3-Zn** = 231 at low CO₂ partial pressures¹², **Mg-MOF-74** and **Zeolite 13X** = 159 and 790, respectively). The high Q_{st} and S_{CM} values exhibited by **TIFSIX-3-Ni**, **NbOFFIVE-1-Ni** and **SIFSIX-3-Ni** suggest potential for utility in CO₂/CH₄ separations.

Experimental breakthrough studies were conducted for CO₂/CH₄ (1/99 and 50/50 v/v) gas mixtures at room temperature. As illustrated in Fig. 2, C and D, CO₂/CH₄ separation was achieved by all six physisorbents examined; CH₄ was eluted through the adsorption bed immediately, whereas CO₂ was retained in the adsorbent bed. For 1/99 CO₂/CH₄ (Fig. 2C and Table 1), **Zeolite 13X** was found to have the highest CO₂ uptake capacity (2.01 mmol g⁻¹). This was closely followed by **TIFSIX-3-Ni** (1.7 mmol g⁻¹) and **NbOFFIVE-1-Ni** (1.61 mmol g⁻¹). MS data revealed that CO₂ concentrations of less than 100 ppm were realized in the outlet effluent for all six physisorbents, affording CH₄ purity of > 99.99% (Fig. 2E). Additionally, **TIFSIX-3-Ni** was found to exhibit even higher CH₄ purity of > 99.995% for ~200 min (effluent CO₂ concentration *ca.* 25 ppm). Upon complete saturation of **TIFSIX-3-Ni**, the sorbent was found to be fully regenerable via desorption of CO₂ at *ca.* 333 K. **NbOFFIVE-1-Ni**, **SIFSIX-3-Ni** and **Zeolite 13X** exhibited comparable uptake capacities of CO₂, however, failed to realise the same levels of CH₄ purity during dynamic breakthrough experiments. **Mg-MOF-74** and **TIFSIX-2-Cu-i** were observed to be the worst performing materials for 1/99 CO₂/CH₄ gas mixtures where selectivity becomes the primary factor.

When the six physisorbents were exposed to the 50/50 CO₂/CH₄ gas mixtures efficient gas separation was once again exhibited by all six physisorbents (Fig. 2D). **Mg-MOF-74**, **Zeolite 13X** and **TIFSIX-2-Cu-i** afforded the highest CO₂ uptake capacities, while **NbOFFIVE-1-Ni**, **TIFSIX-3-Ni** and **SIFSIX-3-Ni** gave lower CO₂ levels in the effluent CH₄ stream. Whereas all six sorbents once again achieved CO₂ effluent concentrations of <100 ppm (Fig. 2F), only **NbOFFIVE-1-Ni**, **TIFSIX-3-Ni** and **SIFSIX-3-Ni** offered CH₄ outlet purities of >99.995% (Table 1). Despite the larger CO₂ uptake capacities of **Mg-MOF-74** and **Zeolite 13X**, they were found to produce CH₄ effluent streams

Table 1. Physicochemical properties, gas sorption and breakthrough data.

Sorbent	Single Component Gas Sorption Studies					Dynamic Breakthrough Experiments			
	S_{BET}^a ($\text{m}^2 \text{g}^{-1}$)	Q_{st} at low loading ^d	CO_2/CH_4 Selectivity 0.01 bar (0.5 bar) ^e	CO_2 uptake 0.01 bar (1.0 bar) ^f	CH_4 uptake 0.01 bar (1.0 bar) ^f	CO_2 uptake from 1/99 $\text{CO}_2/\text{CH}_4^g$	Average Outlet CO_2 ppm ^h	CO_2 uptake from 50/50 $\text{CO}_2/\text{CH}_4^g$	Average Outlet CO_2 ppm ^h
TIFSIX-3-Ni	200 ^b	50.0	3501 (158)	1.995 (2.213)	0.002 (0.220)	1.70	25.1	1.96	37.0
SIFSIX-3-Ni	220 ^b	45.0	1243 (134)	1.808 (2.670)	0.005 (0.299)	1.43	45.6	2.37	40.0
NbOFFIVE-1-Ni	195 ^b	54.0	8482 (366)	2.219 (2.308)	0.004 (0.100)	1.61	52.3	1.83	49.0
TIFSIX-2-Cu-i	590 ^c	35.8	30 (16)	0.260 (4.229)	0.014 (0.760)	0.67	80.0	2.72	75.0
Mg-MOF-74	1100 ^c	42.0	159 (57)	1.409 (7.036)	0.011 (1.007)	1.12	46.7	3.79	78.0
Zeolite 13X	832 ^c	39.0	790 (171)	1.877 (6.060)	0.009 (0.731)	2.01	51.6	3.35	90.0

a) Surface area (m^2/g) calculated from Brunauer-Emmett-Teller (BET) theory; b) Based upon 298 K CO_2 uptake; c) Based upon 77K N_2 uptake; d) Virial fitting of CO_2 sorption data collected between 0-10 mBar; e) CO_2/CH_4 selectivity with ratio of 50:50 and 1:99 at 298 K and 1 bar of total gas pressure, calculated from IAST theory; f) Uptake in mmol g^{-1} at 298 K. Q_{st} and selectivity for materials were determined from dual-site Langmuir-Freundlich equation after fitting the raw data; g) CO_2 uptake (mmol g^{-1}) based upon uptake before CO_2 breakthrough occurs; h) Average outlet CO_2 concentration before breakthrough.

containing CO_2 impurities of 78 and 90 ppm, respectively. The CO_2 capture performance of **TIFSIX-3-Ni** combined with its recyclability (Supporting Information, fig. S52-S53) and previously demonstrated stability data,²¹ suggests potential utility in a one-step process for CO_2 removal from NG during LNG processing regardless of the feed gas CO_2 concentration.

Kinetics are also an important consideration in gas separations and, in order to examine the synergistic nature of the thermodynamics and kinetics for CO_2 capture, CO_2 adsorption kinetic studies were conducted (Fig. S57). Activated samples were exposed to a constant flow of 1.0 bar CO_2 at 308 K. The order of CO_2 uptake at equilibrium was as follows: **Mg-MOF-74** (25 wt. %) > **Zeolite 13X** (19 wt. %) > **TIFSIX-2-Cu-i** (17 wt. %) > **SIFSIX-3-Ni** (ca. 10 wt. %) > **NbOFFIVE-1-Ni** (ca. 10 wt. %) > **TIFSIX-3-Ni** (ca. 10 wt. %). While **NbOFFIVE-1-Ni**, **TIFSIX-3-Ni** and **SIFSIX-3-Ni** exhibited lower CO_2 uptakes, they were found to offer superior kinetics by reaching 90 % of equilibrium loading ca. 1 min after exposure to the CO_2 gas stream. **SIFSIX-3-Ni** and **TIFSIX-3-Ni** were found to exhibit slightly faster uptake rates than that observed for **NbOFFIVE-1-Ni** (Fig. S58).

Removal of CO_2 from NG is one of the most important industrial gas separations and is currently conducted by energy and cost-intensive processes. Although adsorption-based porous materials offer promise to create cost-effective and energy-efficient separation technologies, existing classes of porous materials tend to suffer from a trade-off between adsorption capacity and selectivity or poor kinetics. Additionally, solid physisorbents thus far have lacked the Q_{st} and S_{CM} required to sufficiently reduce the CO_2 concentration in NG for LNG processing across all ranges of composition. We demonstrate herein that a family of HUMs, namely **TIFSIX-3-Ni**, **SIFSIX-3-Ni** and **NbOFFIVE-1-Ni**, can overcome this trade-off and enable highly efficient one-step removal of CO_2 from CH_4 thanks to their ability to exhibit fast adsorption kinetics

and new benchmarks for selectivity. We attribute these results to a combination of high CO_2 adsorption capacity and strong F^-CO_2 interactions. The best performing material, **TIFSIX-3-Ni**, reduced CO_2 levels in the CH_4 outlet gas to as low as 25 ppm (Fig. 2E). Interestingly, despite the lower CH_4 uptake observed for **NbOFFIVE-1-Ni** vs. **TIFSIX-3-Ni** during single-component gas sorption, **TIFSIX-3-Ni** achieved higher levels of CO_2 removal under all mixed gas conditions. This could result from faster uptake kinetics (Fig. S58) in **TIFSIX-3-Ni**, perhaps due to its slightly larger pore aperture than **NbOFFIVE-1-Ni**. While the smaller pore aperture in **NbOFFIVE-1-Ni** could lead to stronger interactions or even a sieving effect, it might also reduce the rate of diffusion of CO_2 into the adsorbent. We attribute the faster kinetic profiles of CO_2 adsorption in **TIFSIX-3-Ni** coupled with its high energy of interaction with CO_2 to be the factors that most contribute to the efficient CO_2/CH_4 separation. Conversely, the larger pore size and reduced F^-CO_2 interactions in **TIFSIX-2-Cu-i** offer significantly reduced S_{CM} of 30. The poor performance of **TIFSIX-2-Cu-i** compared to **TIFSIX-3-Ni** further illustrates how even subtle changes in pore size, pore chemistry and pore geometry can impact F^-CO_2 interactions in HUMs of this type. We attribute the good performance of **Mg-MOF-74** and **Zeolite 13X** to strong M^+CO_2 interactions. The unsaturated Mg^{2+} cations in **Mg-MOF-74** have a smaller ionic radius and a larger ionic valence vs. the extra-framework Na^+ cations in **Zeolite 13X**.²⁷ The presence of exposed metal cations, however, is undesirable if it causes competition with other gas stream constituents. Further, water vapor has previously been shown to strongly coordinate to open metal sites, which competes with CO_2 and can require excessive amounts of energy (>200 °C) to regenerate.²⁸⁻³⁰ In contrast, the breakthrough performance of HUMs for 1/99 and 50/50 mixtures was not observed to decline through 10 successive adsorption/desorption cycles at 353 K (figs. S52-

S53), results which illustrate both the inherent stability and facile recyclability of these HUMs.

In conclusion, we demonstrate that physisorbents can produce ultra-pure CH₄ (>99.995) by efficient removal of CO₂ from both trace (1%) and bulk (50%) concentrations in a one-step process. Single-component gas sorption isotherms suggest that all six physisorbents examined herein are efficient at removing CO₂ from CO₂/CH₄ gas mixtures but the gas separation performance examined by dynamic gas breakthrough experiments reveals that HUMs exhibit superior CO₂ separation performance. Notably, **TIFSIX-3-Ni** reduces CO₂ levels to ca. 25 ppm regardless of the partial pressure of CO₂ in the feed gas and also exhibits fast kinetics. While the S_{CM} of **NbOFFIVE-1-Ni** indicates near sieving performance for CO₂/CH₄ gas mixtures, the narrow pore aperture negatively impacts kinetic CO₂ uptake by the material and as a result reduces overall performance. **TIFSIX-3-Ni** therefore outperforms the other HUM variants in terms of working capacity and kinetics. We also note that **TIFSIX-3-Ni** is particularly facile to prepare by slurry or mechanochemistry and that the method of preparation does not impact gas adsorption performance (Figs. S55, S56). This work further illustrates how study of even the most subtle changes in pore structure and pore chemistry in HUMs can enable significant changes in CO₂ capture performance, in this case for perhaps the most commercially relevant of carbon capture applications.

M.J.Z. acknowledges SFI (13/RP/B2549). M. J. Z. and M. K. acknowledge QNRF (NPRP10-0107-170119). T.P., K.A.F., and B.S. acknowledges the National Science Foundation (Award No. DMR-1607989), including support from the Major Research Instrumentation Program (Award No. CHE-1531590). Computational resources were made available by a XSEDE Grant (No. TG-DMR090028) and by Research Computing at the University of South Florida. T.P. and B.S. also acknowledges support from a ACS Petroleum Research Fund grant (ACS PRF 56673-ND6).

Conflicts of interest

There are no conflicts to declare.

Notes and references

- S. Kitagawa, *Angew. Chem. Int. Ed.*, 2015, **54**, 10686-10687.
- S. Jackson, O. Eiksund and E. Brodal, *Ind. Eng. Chem. Res.*, 2017, **56**, 3388-3398.
- E. Mobil, *2017 Outlook for Energy: A View to 2040*, Irving, Texas, 2017.
- W. Lim, K. Choi and I. Moon, *Ind. Eng. Chem. Res.*, 2013, **52**, 3065-3088.
- Wood, K. et al. Guidebook to gas interchangeability and gas quality (2011).
- T. E. Rufford, S. Smart, G. C. Y. Watson, B. F. Graham, J. Boxall, J. C. Diniz da Costa and E. F. May, *J. Petro. Sci. Eng.*, 2012, **94-95**, 123-154.
- I. Lee and I. Moon, *Ind. Eng. Chem. Res.*, 2017, **56**, 2804-2814.
- R. Sabouni, H. Kazemian and S. Rohani, *Environ. Sci. Pollut. Res.*, 2014, **21**, 5427-5449.
- D. S. Sholl and R. P. Lively, *Nature*, 2016, **532**, 435-437.
- K. J. Chen, D. G. Madden, T. Pham, K. A. Forrest, A. Kumar, Q. Y. Yang, W. Xue, B. Space, J. J. Perry IV, J. P. Zhang, X. M. Chen and M. J. Zaworotko, *Angew. Chem. Int. Ed.*, 2016, **55**, 10268-10272.
- P. Nugent, Y. Belmabkhout, S. D. Burd, A. J. Cairns, R. Luebke, K. Forrest, T. Pham, S. Ma, B. Space, L. Wojtas, M. Eddaoudi and M. J. Zaworotko, *Nature*, 2013, **495**, 80-84.
- Y. Belmabkhout, P.M. Bhatt, K. Adil, R.S. Pillai, A. Cadiou, A. Shkurenko, G. Maurin, G. Liu, W. J. Koros and M. Eddaoudi, *Nature Energy*, 2018, **3**, 1059-1066.
- A. J. Kidnay, W. R. Parrish and D. G. McCartney, *Fundamentals of natural gas processing*, CRC Press, 2011.
- S. K. Elsaidi, M. H. Mohamed, H. T. Schaef, A. Kumar, M. Lusi, T. Pham, K. A. Forrest, B. Space, W. Xu and G. J. Halder, *Chem. Commun.*, 2015, **51**, 15530-15533.
- O. Shekha, Y. Belmabkhout, K. Adil, P. M. Bhatt, A. J. Cairns and M. Eddaoudi, *Chem. Commun.*, 2015, **51**, 13595-13598.
- K. J. Chen, H. S. Scott, D. G. Madden, T. Pham, A. Kumar, A. Bajpai, M. Lusi, K. A. Forrest, B. Space, J. J. Perry and M. J. Zaworotko, *Chem*, 2016, **1**, 753-765.
- A. Cadiou, K. Adil, P. Bhatt, Y. Belmabkhout and M. Eddaoudi, *Science*, 2016, **353**, 137-140.
- S. R. Caskey, A. G. Wong-Foy and A. J. Matzger, *J. Am. Chem. Soc.*, 2008, **130**, 10870-10871.
- J. S. Lee, J. H. Kim, J. T. Kim, J. K. Suh, J. M. Lee and C. H. Lee, *J. Chem. Eng. Data.*, 2002, **47**, 1237-1242.
- A. Kumar, C. Hua, D. G. Madden, D. O'Nolan, K. J. Chen, L. J. Keane, J. J. Perry and M. J. Zaworotko, *Chem. Commun.*, 2017, **53**, 5946-5949.
- J. Liu, P. K. Thallapally, B. P. McGrail, D. R. Brown and J. Liu, *Chem. Soc. Rev.*, 2012, **41**, 2308-2322.
- F. Su and C. Lu, *Eng. Env. Sci.*, 2012, **5**, 9021-9027.
- F. B. Cortés, F. Chejne, F. Carrasco-Marín, C. Moreno-Castilla and A. F. Pérez-Cadenas, *Adsorption*, 2010, **16**, 141-146.
- A. Ziaee, D. Chovan, M. Lusi, J. J. Perry, M. J. Zaworotko and S. A. M. Tofail, *Cryst. Grow. Des.*, 2016, **16**, 3890-3897.
- A. Myers and J. M. Prausnitz, *AIChE*, 1965, **11**, 121-127.
- Z. Bao, L. Yu, Q. Ren, X. Lu and S. Deng, *J. Colloid Interf. Sci.*, 2011, **353**, 549-556.
- N. C. Burtch, H. Jasuja and K. S. Walton, *Chem. Rev.*, 2014, **114**, 10575-10612.
- A. Kumar, D. G. Madden, M. Lusi, K. J. Chen, E. A. Daniels, T. Curtin, J. J. t. Perry and M. J. Zaworotko, *Angew. Chem. Int. Ed.*, 2015, **54**, 14372-14377.
- A. Cadiou, Y. Belmabkhout, K. Adil, P. M. Bhatt, R. S. Pillai, A. Shkurenko, C. Martineau-Corcous, G. Maurin and M. Eddaoudi, *Science*, 2017, **356**, 731-735.

